Project 3: Conservation Laws and Incompressible Navier-Stokes

AE 523, Computational Fluid Dynamics, Fall 2018
Runda Ji

I. Traffic Flow

For traffic flow we have,

$$\frac{\partial \rho}{\partial t} + \frac{\partial f}{\partial x} = 0 \tag{1}$$

where the flux can be written as,

$$f = \rho u_{max}\left(1 - \frac{\rho}{\rho_{max}}\right) \tag{2}$$

with $u_{max} = 1$ and $\rho_{max} = 1$. The initial condition is given by,

$$\rho(x,0) = \begin{cases} \frac{1}{2}\rho_{max} & x < -1 \\ \rho_{max} & -1 \leq x \leq 0 \\ 0 & x > 0 \end{cases} \tag{3}$$

For clarity, the initial condition is depicted in figure 1.

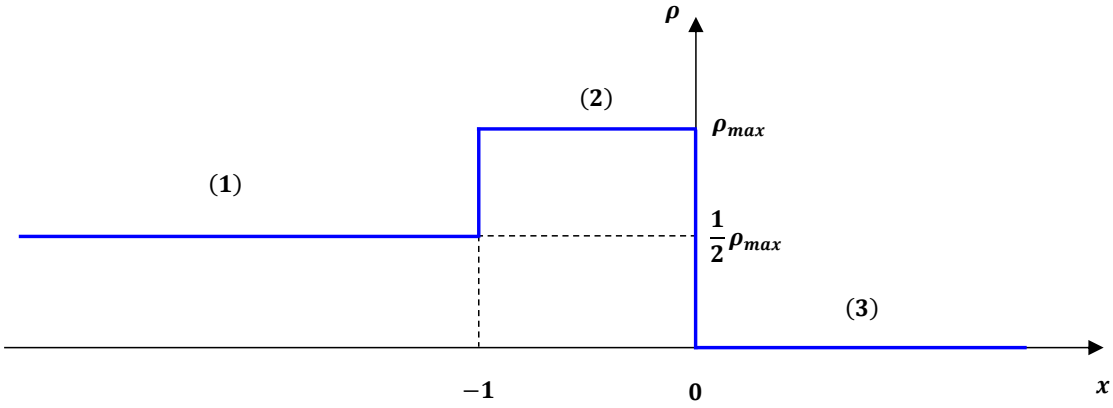

Figure 1. Initial Condition

1. *Characteristics*

The characteristic speed a is given by,

$$\begin{aligned} a &= \frac{df(\rho)}{d\rho} \\ &= \frac{d}{d\rho}\left[u_{max}\left(\rho - \frac{\rho^2}{\rho_{max}}\right)\right] \\ &= u_{max}\left(1 - \frac{2\rho}{\rho_{max}}\right) \end{aligned} \tag{4}$$

Since we have $u_{max} = 1$, $\rho_{max} = 1$, equation 4 reduce to,

$$a = 1 - 2\rho \tag{5}$$

Thus,

$$a = \begin{cases} 0 & \rho = \frac{1}{2} \\ -1 & \rho = 1 \\ 1 & \rho = 0 \end{cases} \tag{6}$$

Note that a shock will form between region (1) and region (2), and the shock speed is given by,

$$s = \frac{f_L - f_R}{\rho_L - \rho_R} \tag{7}$$

Initially, we have $\rho_L = \frac{1}{2}$, $\rho_R = 1$. Consequently,

$$\begin{aligned} f_L &= \rho_L(1 - \rho_L) = \frac{1}{4} \\ f_R &= \rho_R(1 - \rho_R) = 0 \end{aligned} \tag{8}$$

So the initial shock speed $s_0 = -\frac{1}{2}$. Meanwhile, The position of shock can be written as,

$$\begin{aligned} x_s &= x_0 + s_0 \cdot t \\ &= -1 - \frac{1}{2} \cdot t \end{aligned} \tag{9}$$

Note that equation (9) is only valid for $0 \leq t \leq 2$. When $t > 2$, the state on the right hand side is no longer $\rho = 1$, and it is determined by the rarefaction region. The density distribution within the rarefaction can be expressed as,

$$\begin{aligned} \rho_R = \rho(x,t) &= 1 - \frac{x+t}{2t} \\ &= \frac{1}{2} - \frac{1}{2}\frac{x}{t} \end{aligned} \tag{10}$$

Hence,

$$\begin{aligned} f_R &= \rho_R(1 - \rho_R) \\ &= \left(\frac{1}{2} - \frac{1}{2}\frac{x}{t}\right)\left(1 - \frac{1}{2} + \frac{1}{2}\frac{x}{t}\right) \\ &= \left(\frac{1}{2} - \frac{1}{2}\frac{x}{t}\right)\left(\frac{1}{2} + \frac{1}{2}\frac{x}{t}\right) \\ &= \left(\frac{1}{4} - \frac{1}{4}\frac{x^2}{t^2}\right) \end{aligned} \tag{11}$$

Thus, equation (7) can be re-written as,

$$\begin{aligned} s = \frac{dx_s}{dt} &= \frac{f_L - f_R}{\rho_L - \rho_R} \\ &= \frac{\frac{1}{4} - \frac{1}{4} + \frac{1}{4}\frac{x_s^2}{t^2}}{\frac{1}{2} - \frac{1}{2} + \frac{1}{2}\frac{x_s}{t}} \\ &= \frac{\frac{1}{4}\frac{x_s^2}{t^2}}{\frac{1}{2}\frac{x_s}{t}} \\ &= \frac{1}{2}\frac{x_s}{t} \end{aligned} \tag{12}$$

i.e.

$$\begin{aligned} 2\frac{dx_s}{x_s} &= \frac{dt}{t} \\ 2\frac{d(-x_s)}{-x_s} &= \frac{dt}{t} \\ 2\ln(-x_s) &= \ln(t) + C_0 \\ (-x_s)^2 &= C_1 \cdot t \end{aligned} \tag{13}$$

Note that when $t = 2$, $x_s = -2$, so $C_1 = 2$. So, when $t > 2$ we have,

$$x_s = -\sqrt{2t} \tag{14}$$

The characteristics are depicted in figure 2, where the black line represents the shock, while the red lines are the characteristic lines within the rarefaction region.

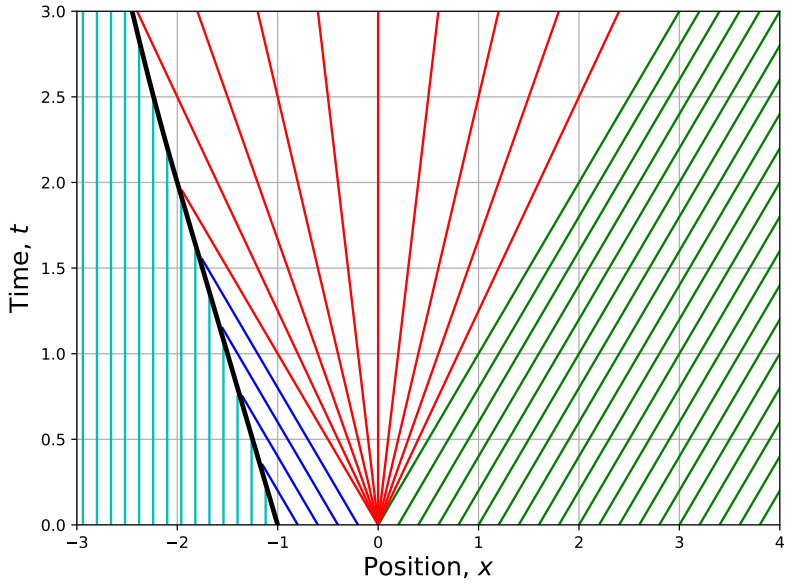

Figure 2. Characteristics of the traffic flow

2. Density Distribution, exact solution

(1) When $t < 2$,

$$\rho(x) = \begin{cases} \frac{1}{2}, & x < -\frac{t}{2} - 1 \\ 1, & -\frac{t}{2} - 1 \le x \le -t \\ \frac{1}{2} - \frac{1}{2}\frac{x}{t}, & -t < x \le t \\ 0, & x > t \end{cases} \tag{15}$$

(2) Similarly when $t \ge 2$, we have,

$$\rho(x) = \begin{cases} \frac{1}{2}, & x < -\sqrt{2t} \\ \frac{1}{2} - \frac{1}{2}\frac{x}{t}, & -\sqrt{2t} \le x \le t \\ 0, & x > t \end{cases} \tag{16}$$

The density distribution at $t = 1$, $t = 2$ and $t = 3$ are plotted in figure 3.

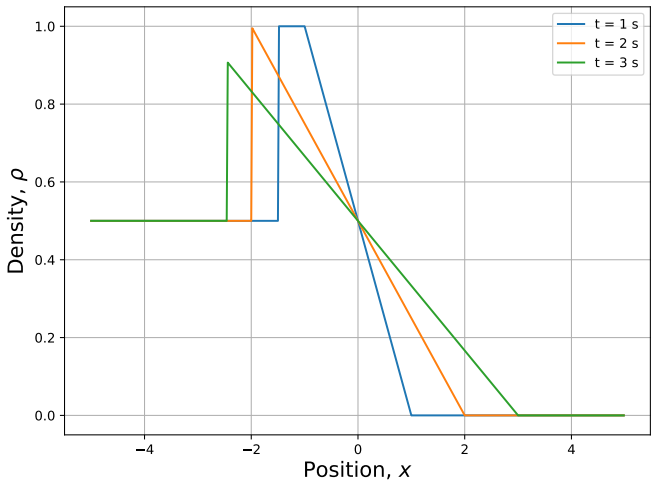

Figure 3. Density distribution, analytical solution.

3. Numerical solution based on the Godunov flux

The Godunov flux is given by,

$$\hat{F}^{G}_{j+\frac{1}{2}} = \begin{cases} \min\limits_{\rho\in[\rho_j,\rho_{j+1}]} f(\rho), & \rho_j < \rho_{j+1} \\ \max\limits_{\rho\in[\rho_j+1,\rho_j]} f(\rho), & \rho_j > \rho_{j+1} \end{cases} \tag{17}$$

The update formula can be expressed as,

$$\rho_j^{n+1} = \rho_j^n + \frac{\Delta t}{\Delta x} \cdot (F_{j-\frac{1}{2}} - F_{j+\frac{1}{2}}) \tag{18}$$

where $\Delta x = 0.01$, $\Delta t = 0.8\Delta x/u_{max}$.

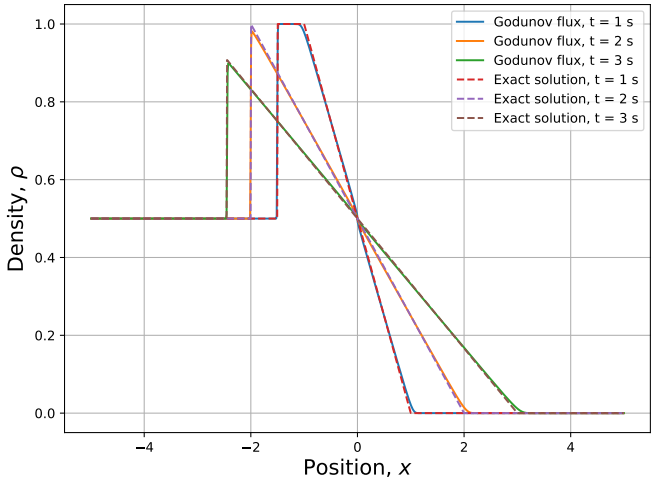

Figure 4. Density distribution, comparison between the Godunov flux and analytic solution.

Implementing the Godunov flux described in equation (17), we can obtain a numerical solution of the density distribution for $t = 1$, $t = 2$ and $t = 3$. As we can see in figure 4, the numerical solution when using the Godunov flux is in good accordance with the exact solution.

4. Numerical solution based on the Roe flux

The Roe flux can be expressed as,

$$\hat{F}_{j+\frac{1}{2}} = \frac{1}{2}(f_i + f_{i+1}) - \frac{1}{2}|\hat{a}_{j+\frac{1}{2}}|(u_{j+1} - u_j) \tag{19}$$

where, the wave speed $\hat{a}_{j+\frac{1}{2}}$ can be expressed as,

$$\hat{a}_{j+\frac{1}{2}} = \frac{f_{j+1} - f_j}{u_{j+1} - u_j} \tag{20}$$

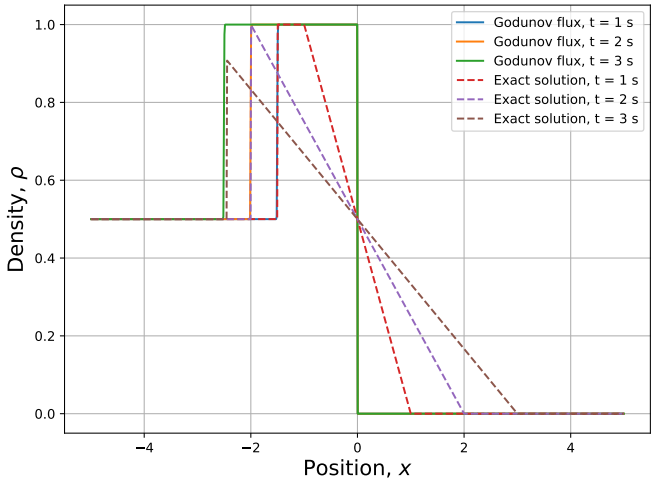

Figure 5. Density distribution, comparison between the Roe flux and analytic solution.

As depicted in figure 5, an expansion shock has occurred in our solution. This non-physical expansion shock is entropy-violating, so we need to apply the entropy fix to generate an entropy satisfying solution.

5. Numerical solution based on the Roe flux, with entropy fix

In order to eliminate the expansion shock shown in figure 5, we need to implement the entropy fix for the Roe flux. Specifically, if $|\lambda| < \epsilon$ then,

$$\lambda = \frac{\epsilon^2 + \lambda^2}{2\epsilon} \tag{21}$$

Generally, λ represent the eigenvalues of matrix $\frac{\partial \mathbf{F}}{\partial \mathbf{u}}(\mathbf{u}^*)$. In our case, the matrix $\frac{\partial \mathbf{F}}{\partial \mathbf{u}}(\mathbf{u}^*)$ reduce to scalar a. Therefore, the entropy fix can be re-written as,

$$a = \frac{\epsilon^2 + a^2}{2\epsilon} \tag{22}$$

if $|a| < \epsilon$. Note that $\epsilon = 0.05 u_{max} = 0.05$.

The numerical solution using Roe flux with entropy fix is depicted in figure 6. Generally speaking, the numerical solution is in accordance with the exact solution. However, near the origin where $x = 0$ and $t = 0$, the wave speed predicted by the numerical solution is lower than the exact solution.

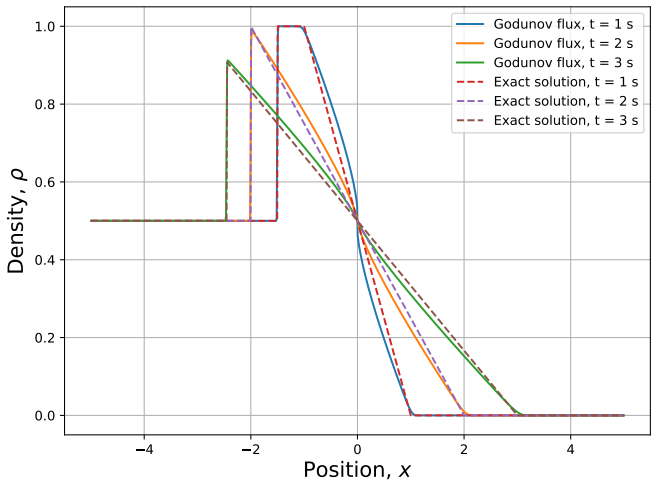

Figure 6. Density distribution, comparison between the Roe flux with entropy fix and analytic solution.

II. Incompressible Flow over a Backward Step

A. Conservation equations

The 2-D incompressible N-S equations is given by,

$$\begin{aligned} \frac{\partial u}{\partial t} + \frac{\partial}{\partial x}(F+p) + \frac{\partial H^x}{\partial y} = 0 \\ \frac{\partial v}{\partial t} + \frac{\partial H^y}{\partial x} + \frac{\partial}{\partial y}(G+p) = 0 \end{aligned} \tag{23}$$

where, the fluxes can be expressed as,

$$\begin{aligned} F &= u^2 - \nu\frac{\partial u}{\partial x} \\ G &= v^2 - \nu\frac{\partial v}{\partial y} \\ H^x &= uv - \nu\frac{\partial u}{\partial y} \\ H^y &= uv - \nu\frac{\partial v}{\partial x} \end{aligned} \tag{24}$$

The discretized version of equation (24) will be given in equation (32) later on.

B. Computational domain

The computational domain and the staggered storage are illustrated in figure 7. As shown in figure 7, there is a layer of yellow cells outside the $N_x \times N_y$ domain. Those yellow cells around represent the ghost cells, and we need those ghost cells when implementing the boundary conditions.

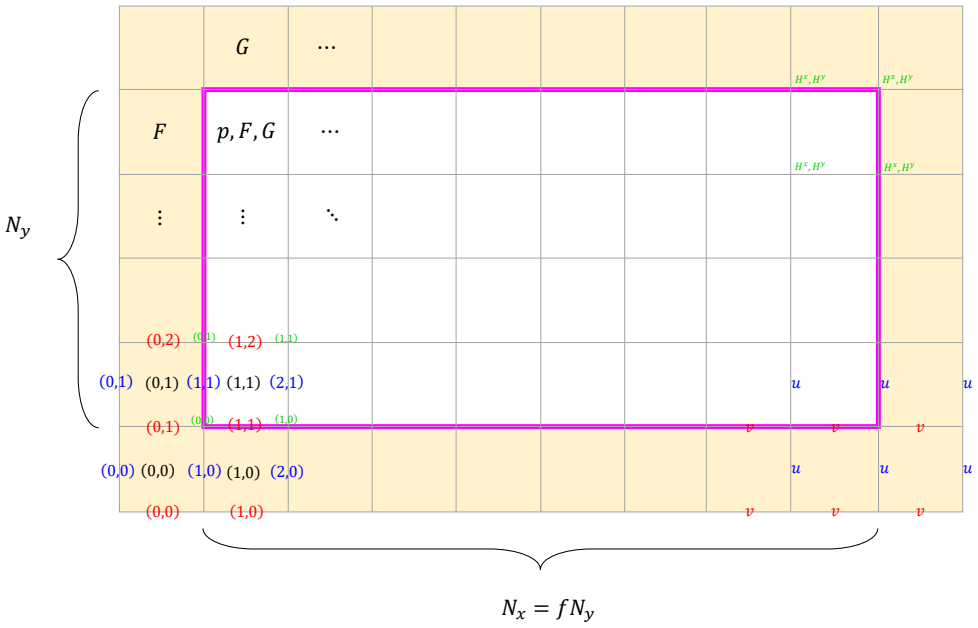

Figure 7. Computational domain and the storage of the data.

As shown in figure 7, p,F and G are stored in the cell centers, while H^x and H^y are stored at the nodes of the grid. Note that the indices start from 0. Specifically, (0,0) represents the ghost cell located at the lower-left corner, while (i,j), (i,j) and (i,j) are the indices of the vertical edges, horizontal edges and the nodes, respectively.

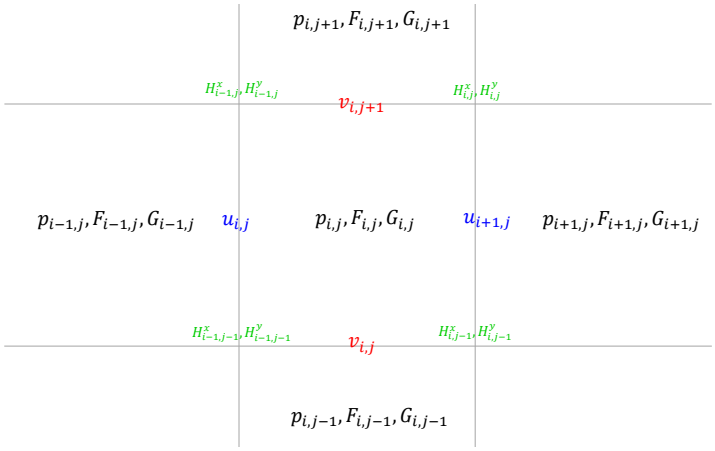

Figure 8. Edges and nodes around cell (i,j).

The indices of nodes and edges around cell(i,j) are shown in figure 8. Note that there is a shift of indices for coding. Specifically, $u_{i,j}$ and $u_{i+1,j}$ in our code correspond to $u_{i-\frac{1}{2},j}$ and $u_{i+\frac{1}{2},j}$ in the literature. Meanwhile, $v_{i,j}$ and $v_{i,j+1}$ represent $v_{i,j-\frac{1}{2}}$ and $v_{i,j+\frac{1}{2}}$ in the literature. Additionally, $H^x_{i,j}$ and $H^y_{i,j}$ in our code are identical to $H^x_{i+\frac{1}{2},j+\frac{1}{2}}$,$H^y_{i+\frac{1}{2},j+\frac{1}{2}}$ in the lecture note.

C. Boundary conditions

1. *Wall condition*

As shown in figure 9, at the upper and lower boundary, the no slip condition requires the tangential velocity to match the wall velocity, which is zero, i.e.

$$\begin{aligned} u_{w,up} = 0 \Rightarrow \frac{u_{i,N_y+1} + u_{i,N_y}}{2} = 0 \Rightarrow u_{i,N_y+1} = -u_{i,N_y} \\ u_{w,low} = 0 \Rightarrow \frac{u_{i,1} + u_{i,0}}{2} = 0 \Rightarrow u_{i,0} = -u_{i,1} \end{aligned} \tag{25}$$

Meanwhile, the zero flow-through requires the normal fluid velocity to be zero,

$$\begin{aligned} v_{i,N_y+1} = v_{i,N_y+2} = 0 \\ v_{i,1} = v_{i,0} = 0 \end{aligned} \tag{26}$$

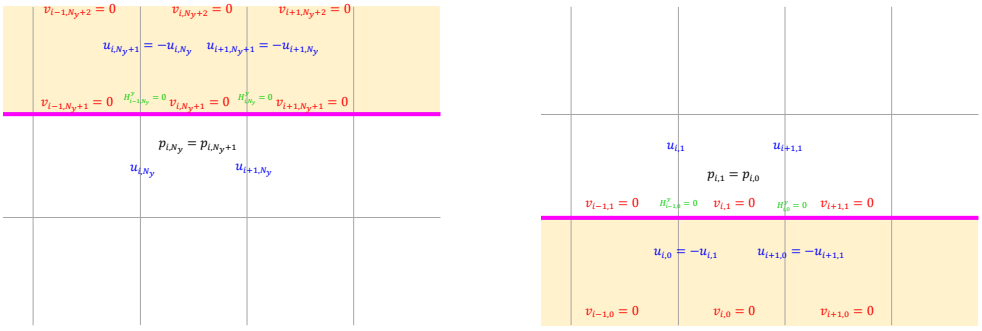

Figure 9. Boundary conditions at the upper and lower wall

The pressure boundary condition is $p_{i,N_y} = p_{i,N_y+1}$ and $p_{i,1} = p_{i,0}$ for the upper and lower wall, respectively.

Similarly, as for the wall boundary condition on the left hand side,

$$\begin{aligned} v_{0,j} = -v_{1,j} \\ u_{1,j} = u_{0,j} = 0 \\ p_{1,j} = p_{0,j} \end{aligned} \tag{27}$$

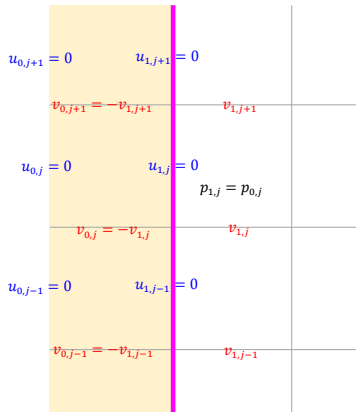

Figure 10. Boundary conditions at the left wall

2. Inflow and outflow condition

Now consider the inflow and outflow boundary condition, where the horizontal velocity are given (parabolic profile), while the vertical velocity is zero. Specifically, the parabolic velocity profile can be written as,

$$u_{in} = -(y-h)(y-2h) \cdot \frac{4U_0}{h^2} \tag{28}$$

Note that the value of equation (30) is evaluated at the mid-point of each interval. Specifically, for the j^{th} interval on the left inflow boundary, $y_j = (j - \frac{1}{2})\Delta y$, hence,

$$\begin{aligned} u_{0,j} = u_{1,j} &= -(y_j - h)(y_j - 2h) \cdot \frac{4U_0}{h^2} \\ &= -\left[\left(j - \frac{1}{2}\right)\Delta y - h\right] \cdot \left[\left(j - \frac{1}{2}\right)\Delta y - 2h\right] \cdot \frac{4U_0}{h^2} \end{aligned} \tag{29}$$

Similarly, as for the outflow condition,

$$u_{out} = -(y-0)(y-2h) \cdot \frac{U_0}{2h^2} \tag{30}$$

Thus,

$$\begin{aligned} u_{N_x+1,j} = u_{N_x+2,j} &= -(y_j - 0)(y_j - 2h) \cdot \frac{U_0}{2h^2} \\ &= -\left(j - \frac{1}{2}\right)\Delta y \cdot \left[\left(j - \frac{1}{2}\right)\Delta y - 2h\right] \cdot \frac{U_0}{2h^2} \end{aligned} \tag{31}$$

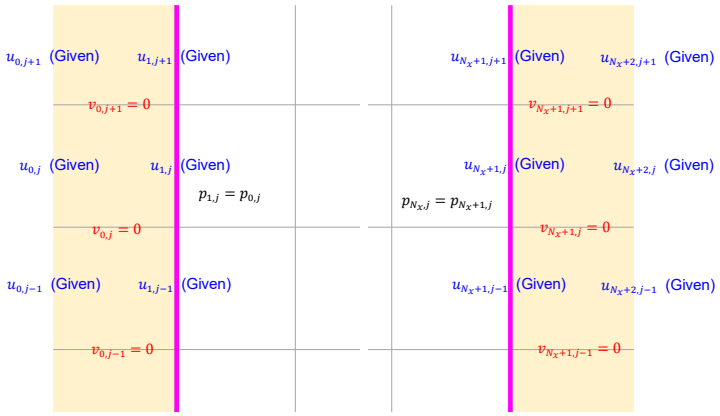

Figure 11. Inflow and outflow boundary conditions

D. Projection method implementation

1. Calculate the fluxes

The fluxes are calculated based on the current velocity field.

$$\begin{aligned} F_{i,j} &= F_{convec} - \frac{\nu}{\Delta}(u_{i+1,j} - u_{i,j}) \\ G_{i,j} &= G_{convec} - \frac{\nu}{\Delta}(v_{i,j+1} - v_{i,j}) \\ H^x_{i,j} &= H^x_{convec} - \frac{\nu}{\Delta}(u_{i+1,j+1} - u_{i+1,j}) \\ H^y_{i,j} &= H^y_{convec} - \frac{\nu}{\Delta}(v_{i+1,j+1} - v_{i,j+1}) \end{aligned} \tag{32}$$

The convective term can be expressed as $f_{convec} = q\phi$, where q is the transport velocity, while ϕ is the transported quantity. $\phi_{i,j}$ is determined by the sign of $q_{i,j}$.

Table 1. Calculate the convective component of the fluxes

Flux	transport velocity q	transported quantity ϕ
F	u	u
G	v	v
H^x	v	u
H^y	u	v

Specifically, in order to compute the convective term in $F_{i,j}$, we need to evaluate,

$$q_{i,j} = \frac{1}{2}(u_{i,j} + u_{i+1,j}) \tag{33}$$

Where $u_{i,j}$ and $u_{i+1,j}$ are stored at the left and right vertical edges of cell (i,j). Then, based on the sign of $q_{i,j}$ we can compute $\phi_{i,j}$ using the following formula,

$$\begin{aligned} \phi_{i,j} &= \frac{3u_{i+1,j} + 6u_{i,j} - u_{i-1,j}}{8} \text{ if } q_{i,j} > 0 \\ \phi_{i,j} &= \frac{3u_{i,j} + 6u_{i+1,j} - u_{i+2,j}}{8} \text{ if } q_{i,j} < 0 \end{aligned} \tag{34}$$

The calculation for the convective term in $G_{i,j}$ is quite similar, where we first calculate $q_{i,j} = \frac{1}{2}(v_{i,j} + v_{i,j+1})$, and then compute $\phi_{i,j}$ based on the sign of $q_{i,j}$.

However, calculation for H^x_{convec} and H^y_{convec} is slightly different, since those two values are stored at the nodes rather than stored at the center of cells. To compute the convective term in $H^x_{i,j}$. we first need to calculate $q_{i,j} = \frac{1}{2}(v_{i,j+1} + v_{i+1,j+1})$. Note that $v_{i,j+1}$ and $v_{i+1,j+1}$ are the two horizontal edges beside node (i,j). based on the sign of $q_{i,j}$ we can compute the $\phi_{i,j}$.

$$\begin{aligned} \phi_{i,j} &= \frac{3u_{i+1,j+1} + 6u_{i+1,j} - u_{i+1,j-1}}{8} \text{ if } q_{i,j} > 0 \\ \phi_{i,j} &= \frac{3u_{i+1,j} + 6u_{i+1,j+1} - u_{i+2,j+2}}{8} \text{ if } q_{i,j} < 0 \end{aligned} \tag{35}$$

The calculation for the convective term in $H^y_{i,j}$ is similar to equation (35).

2. Compute the fractional-step velocity field

In this step, we neglect the pressure term in equation (23), thus the update formula can be expressed as,

$$\begin{aligned} u^*_{i,j} &= u^n_{i,j} - \Delta t\left(\frac{\partial F}{\partial x} + \frac{\partial H^x}{\partial y}\right) \\ v^*_{i,j} &= v^n_{i,j} - \Delta t\left(\frac{\partial H^y}{\partial x} + \frac{\partial G}{\partial y}\right) \end{aligned} \tag{36}$$

where $\frac{\partial F}{\partial x}$ and $\frac{\partial H^x}{\partial y}$ are evaluated at the vertical edge $u^n_{i,j}$, thus,

$$\begin{aligned} \frac{\partial F}{\partial x} &= \frac{1}{\Delta x}(F_{i,j} - F_{i-1,j}) \\ \frac{\partial H^x}{\partial y} &= \frac{1}{\Delta y}(H^x_{i-1,j} - H^x_{i-1,j-1}) \end{aligned} \tag{37}$$

Similarity, since $\frac{\partial H^y}{\partial x}$ and $\frac{\partial G}{\partial y}$ are evaluated at the horizontal edge $v^n_{i,j}$,

$$\begin{aligned} \frac{\partial H^y}{\partial x} &= \frac{1}{\Delta x}(H^y_{i,j-1} - H^y_{i-1,j-1}) \\ \frac{\partial G}{\partial y} &= \frac{1}{\Delta y}(G_{i,j} - G_{i,j-1}) \end{aligned} \tag{38}$$

From equation (36), we can obtain the intermediate velocity field u^* and v^*. Then we need to solve the pressure Poisson equation in order to find the pressure field.

3. Solve the pressure Poisson equation

The pressure Poisson equation is given by,

$$\nabla^2 p^{n+1} = \rho \frac{\nabla \cdot \vec{v}^*}{\Delta t} \tag{39}$$

Let $\rho = 1$, equation (39) can be discretized as,

$$\frac{p^{n+1}_{i-1,j} - 2p^{n+1}_{i,j} + p^{n+1}_{i+1,j}}{\Delta x^2} + \frac{p^{n+1}_{i,j-1} - 2p^{n+1}_{i,j} + p^{n+1}_{i,j+1}}{\Delta y^2} = \frac{1}{\Delta t}\left(\frac{u^*_{i+1,j} - u^*_{i,j}}{\Delta x} + \frac{v^*_{i,j+1} - v^*_{i,j}}{\Delta y}\right) \tag{40}$$

Note that we have $\Delta x = \Delta y = \Delta$, thus,

$$p^{n+1}_{i,j-1} + p^{n+1}_{i-1,j} - 4p^{n+1}_{i,j} + p^{n+1}_{i+1,j} + p^{n+1}_{i,j+1} = \frac{\Delta}{\Delta t}(u^*_{i+1,j} - u^*_{i,j} + v^*_{i,j+1} - v^*_{i,j}) \tag{41}$$

In order to solve equation (41), we need to build a matrix system as follows

$$\begin{bmatrix}
-2 & 1 & 0 & \cdots & 1 & 0 & 0 & \cdots & 0 & \cdots & 0 & 0 & 0 & \cdots & 0 & \cdots \\
1 & -3 & 1 & \cdots & 0 & 1 & 0 & \cdots & 0 & \cdots & 0 & 0 & 0 & \cdots & 0 & \cdots \\
0 & 1 & -3 & \cdots & 0 & 0 & 1 & \cdots & 0 & \cdots & 0 & 0 & 0 & \cdots & 0 & \cdots \\
\cdots & \cdots & \cdots & \cdots & \cdots & \cdots & \cdots & \cdots & \cdots & \cdots & \cdots & \cdots & \cdots & \cdots & \cdots & \cdots \\
1 & 0 & 0 & \cdots & -3 & 1 & 0 & \cdots & 0 & \cdots & 0 & 0 & 0 & \cdots & 0 & \cdots \\
0 & 1 & 0 & \cdots & 1 & -4 & 1 & \cdots & 0 & \cdots & 0 & 0 & 0 & \cdots & 0 & \cdots \\
0 & 0 & 1 & \cdots & 0 & 1 & -4 & \cdots & 0 & \cdots & 0 & 0 & 0 & \cdots & 0 & \cdots \\
\cdots & \cdots & \cdots & \cdots & \cdots & \cdots & \cdots & \cdots & \cdots & \cdots & \cdots & \cdots & \cdots & \cdots & \cdots & \cdots \\
0 & 0 & 0 & \cdots & 0 & 0 & 0 & \cdots & -4 & \cdots & 0 & 1 & 0 & \cdots & 0 & \cdots \\
\cdots & \cdots & \cdots & \cdots & \cdots & \cdots & \cdots & \cdots & \cdots & \cdots & \cdots & \cdots & \cdots & \cdots & \cdots & \cdots \\
0 & 0 & 0 & \cdots & 0 & 0 & 0 & \cdots & 0 & \cdots & -4 & 1 & 0 & \cdots & 0 & \cdots \\
0 & 0 & 0 & \cdots & 0 & 0 & 0 & \cdots & 1 & \cdots & 1 & -4 & 1 & \cdots & 1 & \cdots \\
0 & 0 & 0 & \cdots & 0 & 0 & 0 & \cdots & 0 & \cdots & 0 & 1 & -4 & \cdots & 0 & \cdots \\
\cdots & \cdots & \cdots & \cdots & \cdots & \cdots & \cdots & \cdots & \cdots & \cdots & \cdots & \cdots & \cdots & \cdots & \cdots & \cdots \\
0 & 0 & 0 & \cdots & 0 & 0 & 0 & \cdots & 0 & \cdots & 0 & 1 & 0 & \cdots & -4 & \cdots \\
\cdots & \cdots & \cdots & \cdots & \cdots & \cdots & \cdots & \cdots & \cdots & \cdots & \cdots & \cdots & \cdots & \cdots & \cdots & \cdots
\end{bmatrix}
\begin{bmatrix}
p_{1,1} \\ p_{2,1} \\ p_{3,1} \\ \cdots \\ p_{1,2} \\ p_{2,2} \\ p_{3,2} \\ \cdots \\ p_{i,j-1} \\ \cdots \\ p_{i-1,j} \\ p_{i,j} \\ p_{i+1,j} \\ \cdots \\ p_{i,j+1} \\ \cdots
\end{bmatrix}
= \frac{\Delta}{\Delta t}
\begin{bmatrix}
u^*_{2,1} - u^*_{1,1} + v^*_{1,2} - v^*_{1,1} \\
u^*_{3,1} - u^*_{2,1} + v^*_{2,2} - v^*_{2,1} \\
u^*_{4,1} - u^*_{3,1} + v^*_{3,2} - v^*_{3,1} \\
\cdots \\
u^*_{2,2} - u^*_{1,2} + v^*_{1,3} - v^*_{1,2} \\
u^*_{3,2} - u^*_{2,2} + v^*_{2,3} - v^*_{2,2} \\
u^*_{4,2} - u^*_{3,2} + v^*_{3,3} - v^*_{3,2} \\
\cdots \\
u^*_{i+1,j-1} - u^*_{i,j-1} + v^*_{i+1,j} - v^*_{i,j-1} \\
\cdots \\
u^*_{i,j} - u^*_{i-1,j} + v^*_{i-1,j+1} - v^*_{i-1,j} \\
u^*_{i+1,j} - u^*_{i,j} + v^*_{i,j+1} - v^*_{i,j} \\
u^*_{i+2,j} - u^*_{i+1,j} + v^*_{i+1,j+1} - v^*_{i+1,j} \\
\cdots \\
u^*_{i+1,j+1} - u^*_{i,j+1} + v^*_{i,j+2} - v^*_{i,j+1} \\
\cdots
\end{bmatrix} \tag{42}$$

In order to avoid singularity when solving this pressure Poisson equation, we need to replace one of these equations with $p_{i,j} = 0$. In our code, we set the pressure stored in the cell at upper-right corner as zero, i.e. $p_{N_x,N_y} = 0$. Hence the last row of equation (42) need to be modified as,

$$\begin{bmatrix} \cdots & \cdots & \cdots & 1 \end{bmatrix}
\begin{bmatrix} \\ \vdots \\ \\ \vdots \\ \\ p_{N_x,N_y} \end{bmatrix}
= \frac{\Delta}{\Delta t}
\begin{bmatrix} \\ \vdots \\ \\ \vdots \\ \\ 0 \end{bmatrix} \tag{43}$$

4. Correct the velocity field

After the pressure Poisson equation is solved, the velocity field can be corrected.

$$\begin{aligned}
u^{n+1}_{i,j} &= u^*_{i,j} - \frac{\Delta t}{\Delta}(p_{i,j} - p_{i-1,j}) \\
v^{n+1}_{i,j} &= v^*_{i,j} - \frac{\Delta t}{\Delta}(p_{i,j} - p_{i,j-1})
\end{aligned} \tag{44}$$

5. Residual and post-processing

Repetitively run the above steps until the residual reaches 1e-5, where the residual $|R|_{L_1}$ can be expressed as,

$$|R|_{L_1} = \sum_{i=2}^{Nx}\sum_{j=1}^{Ny}|R_{i,j}| + \sum_{i=1}^{Nx}\sum_{j=2}^{Ny}|R_{i,j}| \tag{45}$$

where $|R_{i,j}|$ and $|R_{i,j}|$ correspond to the vertical and horizontal edges, respectively.

$$\begin{aligned}
|R_{i,j}| &= \Delta(F_{i,j} + p_{i,j} - F_{i-1,j} - p_{i-1,j}) + \Delta(H^x_{i-1,j} - H^x_{i-1,j-1}) \\
|R_{i,j}| &= \Delta(G_{i,j} + p_{i,j} - G_{i,j-1} - p_{i,j-1}) + \Delta(H^y_{i,j-1} - H^y_{i-1,j-1})
\end{aligned} \tag{46}$$

After we obtain a converged solution, we need to compute the stream function ψ,

$$\psi(B) - \psi(A) = \int_A^B \vec{v} \cdot \vec{n} ds \tag{47}$$

For $\psi_{I,J}$ at node (I,J), we have,

$$\psi_{I,J} = \sum_{j=1}^{J} u_{I+1,j} \cdot \Delta \tag{48}$$

Note that we set $\psi_{i,0} = 0$ at the lower wall.

E. Results and analysis

The Reynolds number Re is defined as,

$$Re = \frac{2U_0}{3}\frac{2h}{\nu} \tag{49}$$

We have ran our simulation under 3 different Reynolds number, $Re = 100$, $Re = 200$ and $Re = 400$. For each Reynolds number, we ran our code with 2 N_y, $N_y = 16$ and $N_y = 32$. For each N_y, we set $f = N_x/N_y = 6, 8, 12$. So for each Reynolds number we will run our code on $2 \times 3 = 6$ meshes.

As shown in figure 12 and figure 13, the reattachment length is approximately $3.2(x/h)$ when $Re = 100$. We can see that for $Re = 100$, setting the domain length as $f = 6$ is long enough for the flow to become fully developed. Comparing figure 12 with figure 14, we can see that the secondary vortex at the lower-left corner was not detected when using $N_y = 16$ mesh. However when we shift to $N_y = 32$ mesh, we can see that vortex at the corner.

1. *Re=100*

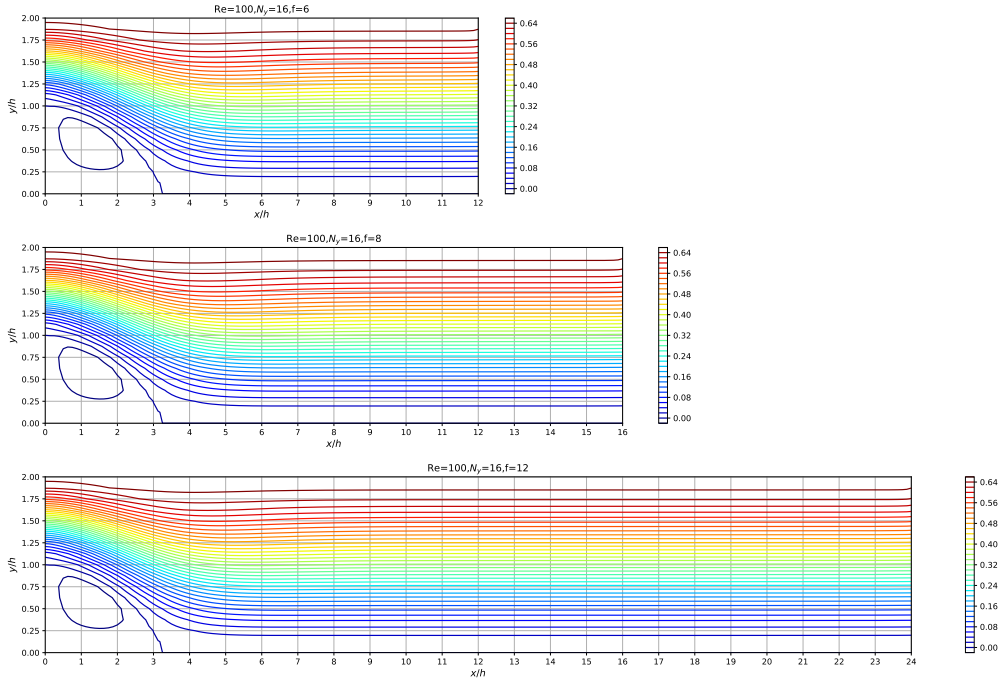

Figure 12. Stream line of $Re = 100$, $N_y = 16$, $f = 6, 8, 12$.

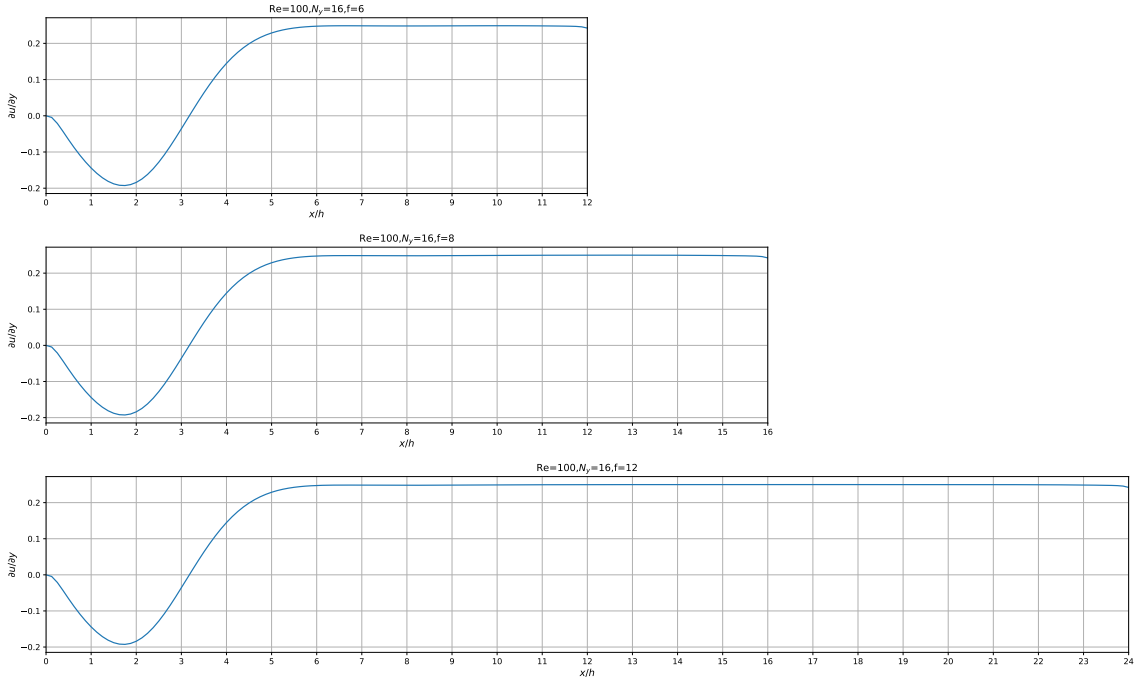

Figure 13. $\partial u/\partial y$ **of** $Re = 100$**,** $N_y = 16$**,** $f = 6, 8, 12$**.**

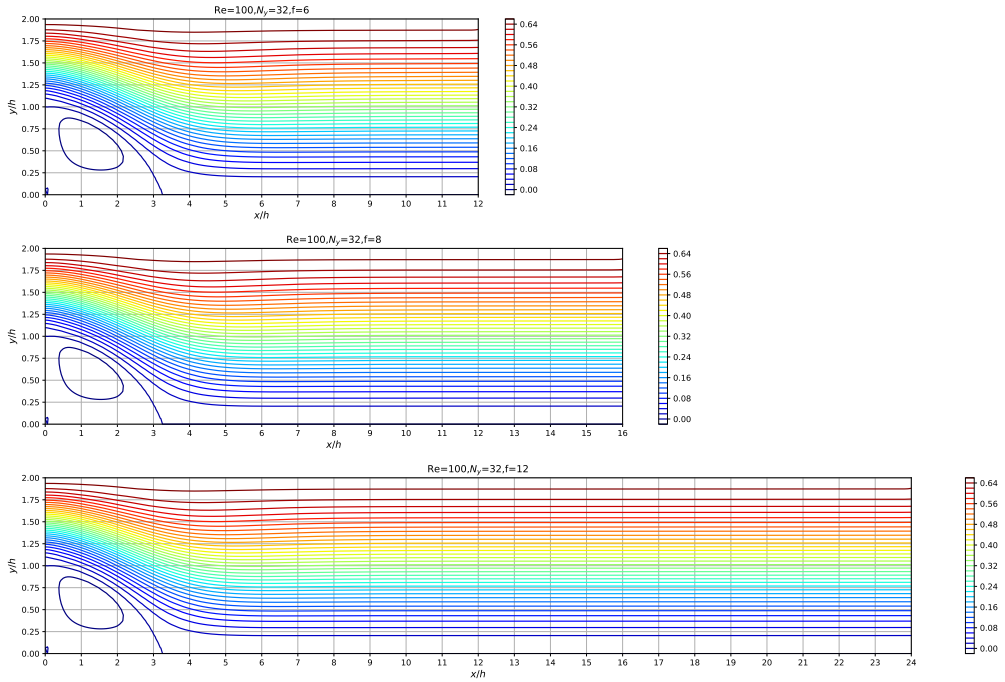

Figure 14. Stream line of $Re = 100$**,** $N_y = 32$**,** $f = 6, 8, 12$**.**

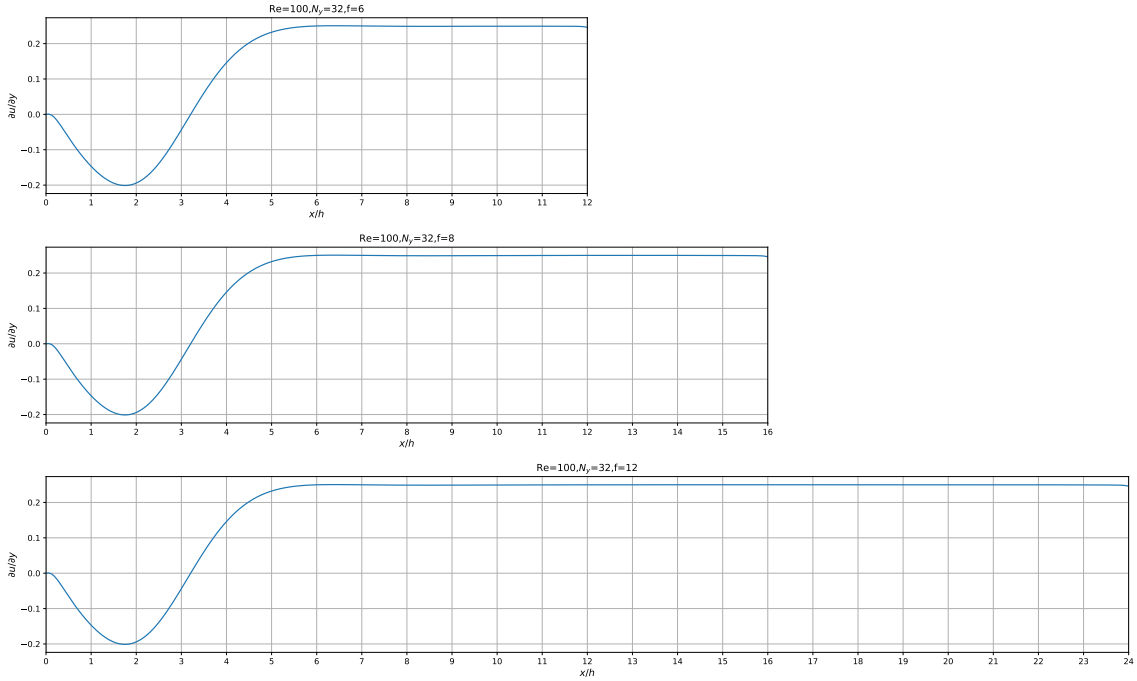

Figure 15. $\partial u/\partial y$ **of** $Re = 100$**,** $N_y = 16$**,** $f = 6, 8, 12$**.**

2. Re=200

When we increase Reynolds number to $Re = 200$, we can clearly see that the reattachment length has also increase to $5.2(x/h)$.

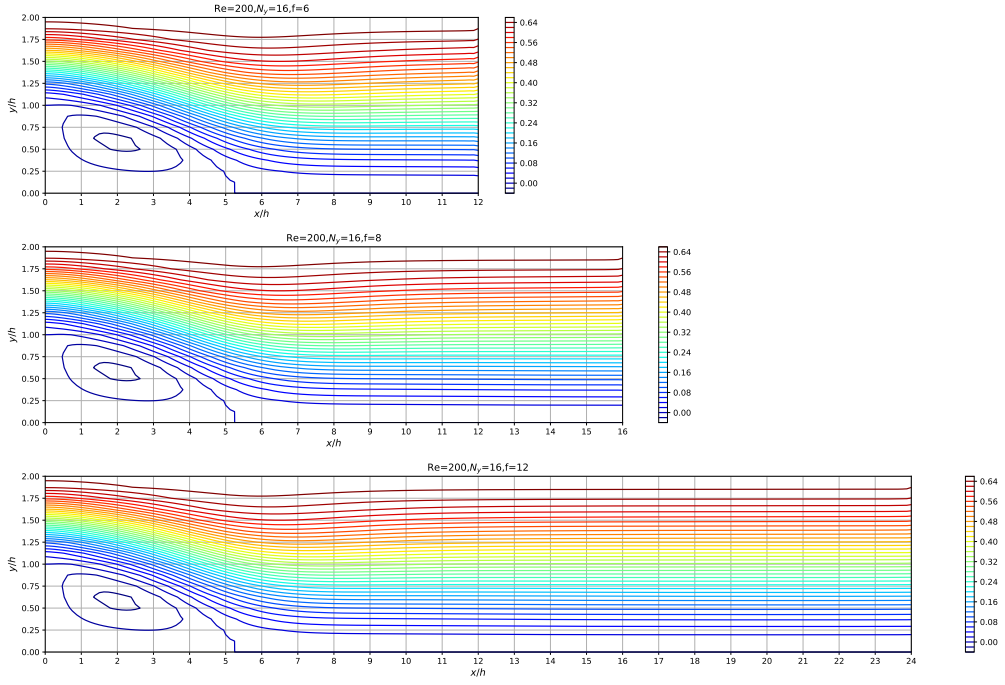

Figure 16. Stream line of $Re = 200$**,** $N_y = 16$**,** $f = 6, 8, 12$**.**

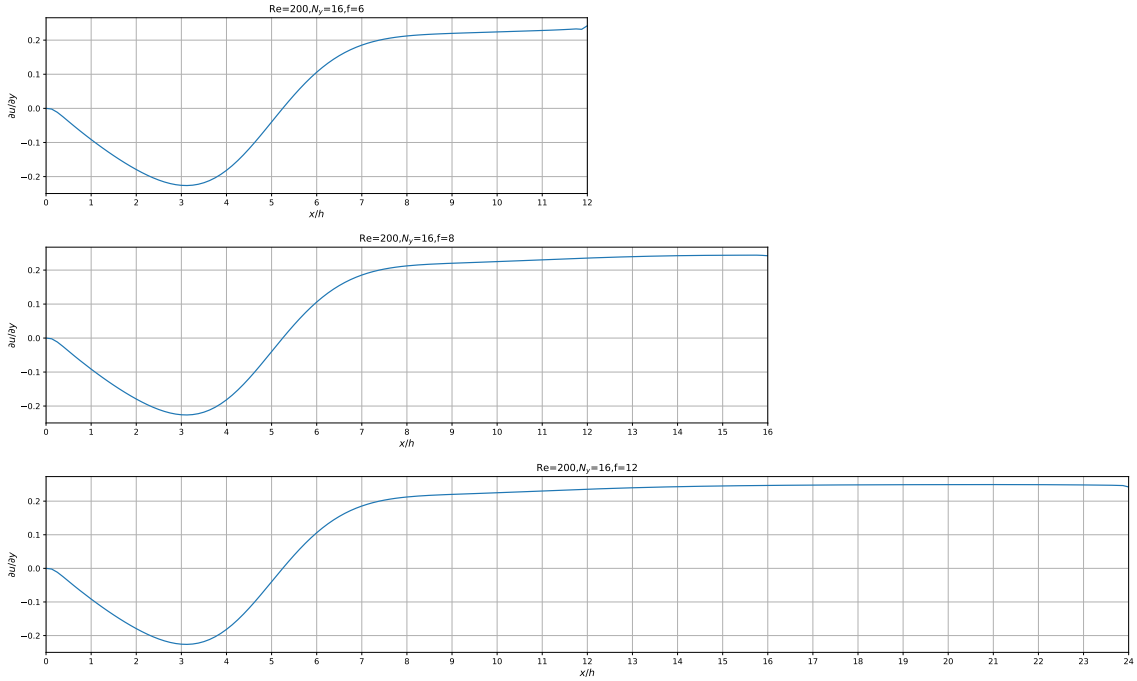

Figure 17. $\partial u/\partial y$ **of** $Re = 200$**,** $N_y = 16$**,** $f = 6, 8, 12$**.**

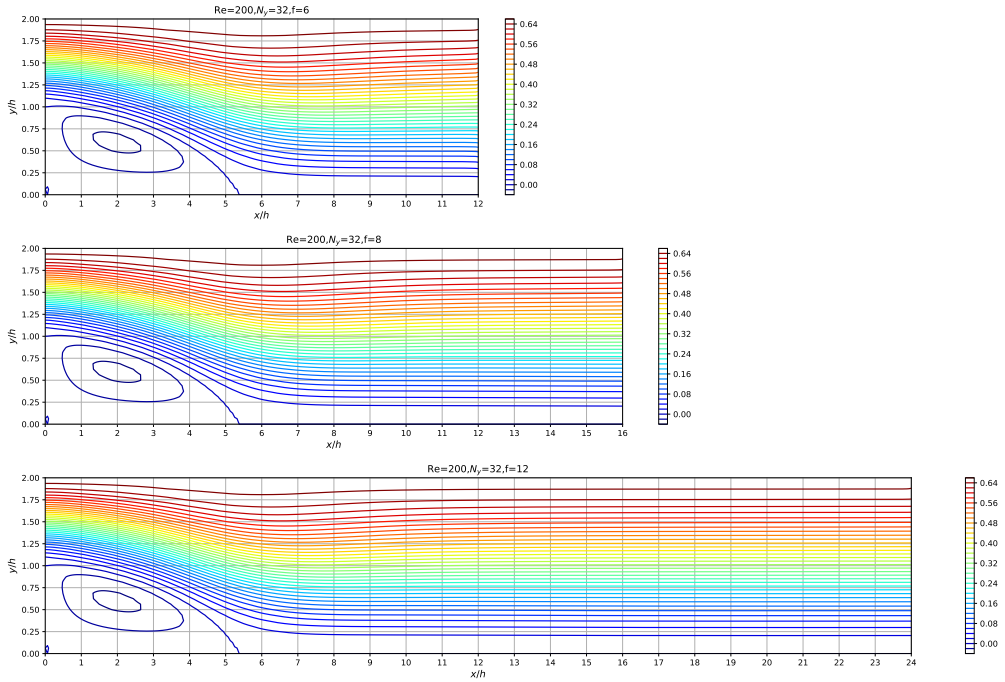

Figure 18. Stream line of $Re = 200$**,** $N_y = 32$**,** $f = 6, 8, 12$**.**

Similar to figure 14, as shown in figure 18, when running the simulation on a mesh with higher resolution, we can detect that secondary vortex at the lower-left corner.

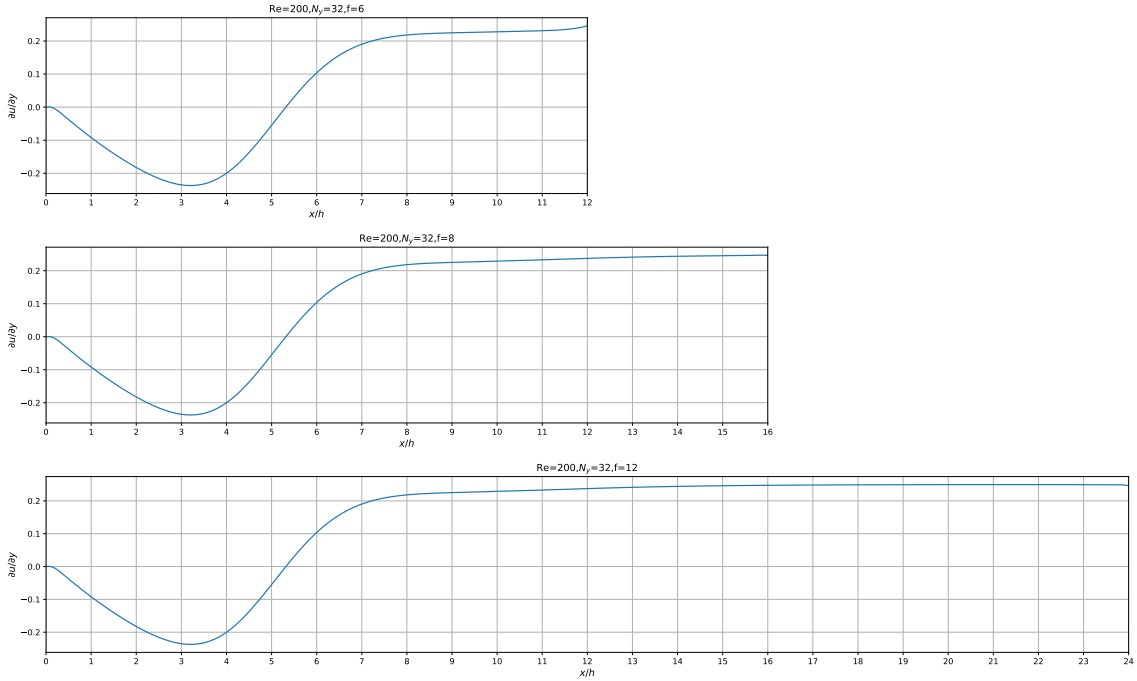

Figure 19. $\partial u/\partial y$ **of** $Re = 200$**,** $N_y = 16$**,** $f = 6, 8, 12$**.**

3. Re=400

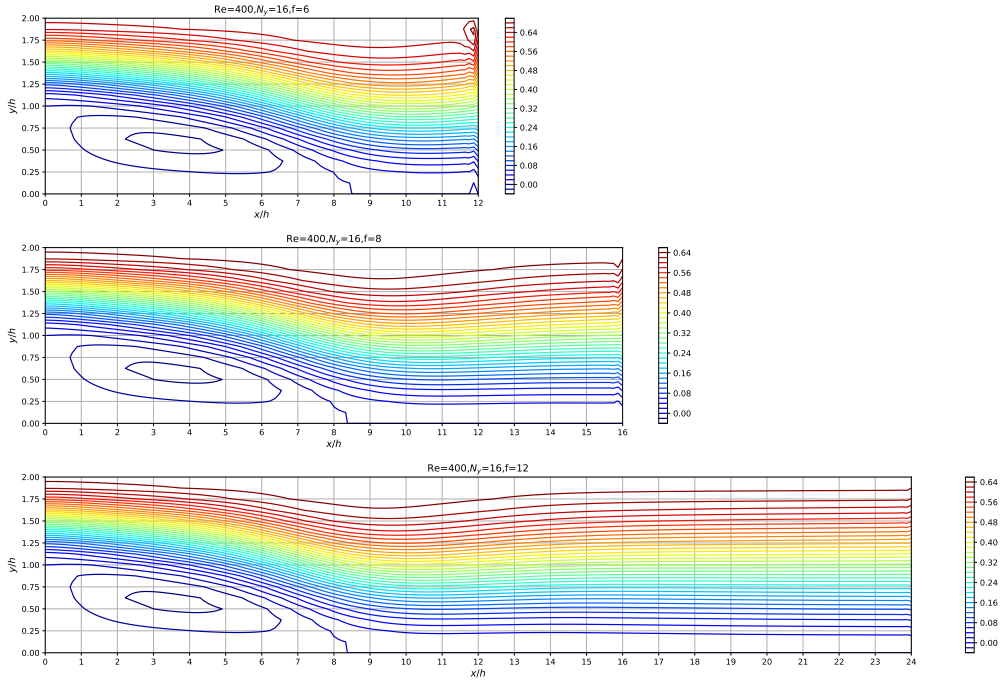

Figure 20. Stream line of $Re = 400$**,** $N_y = 16$**,** $f = 6, 8, 12$**.**

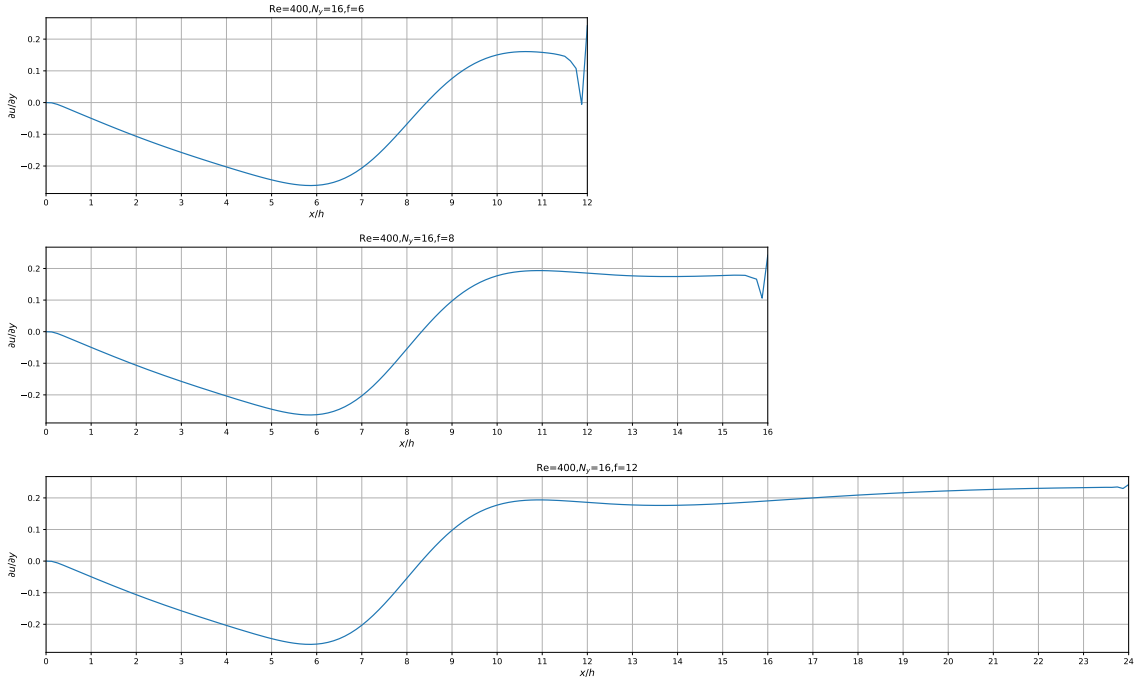

Figure 21. $\partial u/\partial y$ **of** $Re = 400$**,** $N_y = 16$**,** $f = 6, 8, 12$**.**

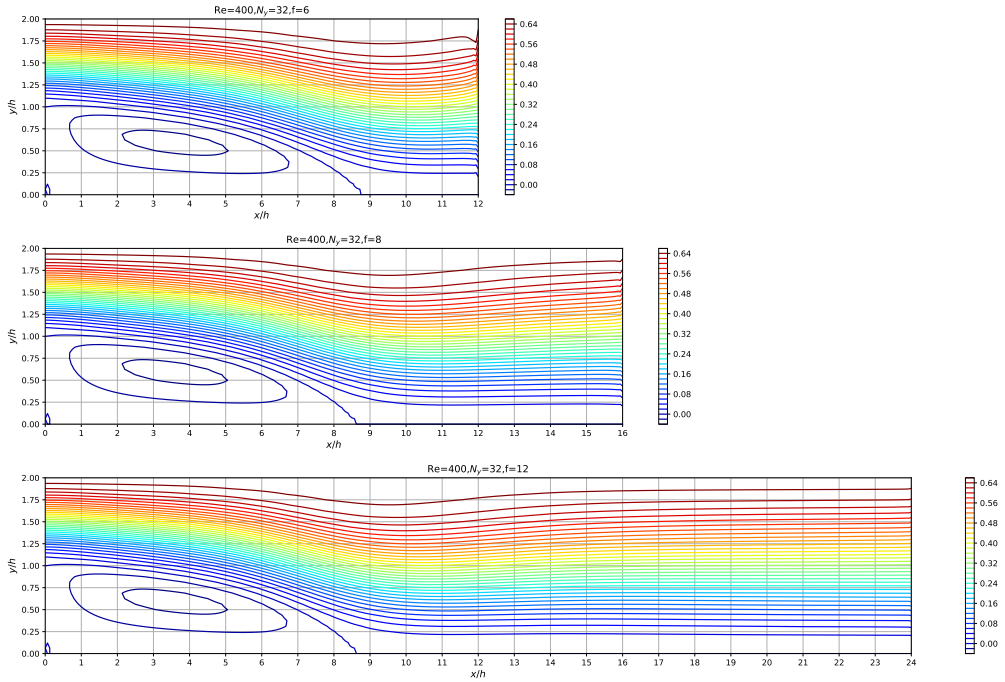

Figure 22. Stream line of $Re = 400$**,** $N_y = 32$**,** $f = 6, 8, 12$**.**

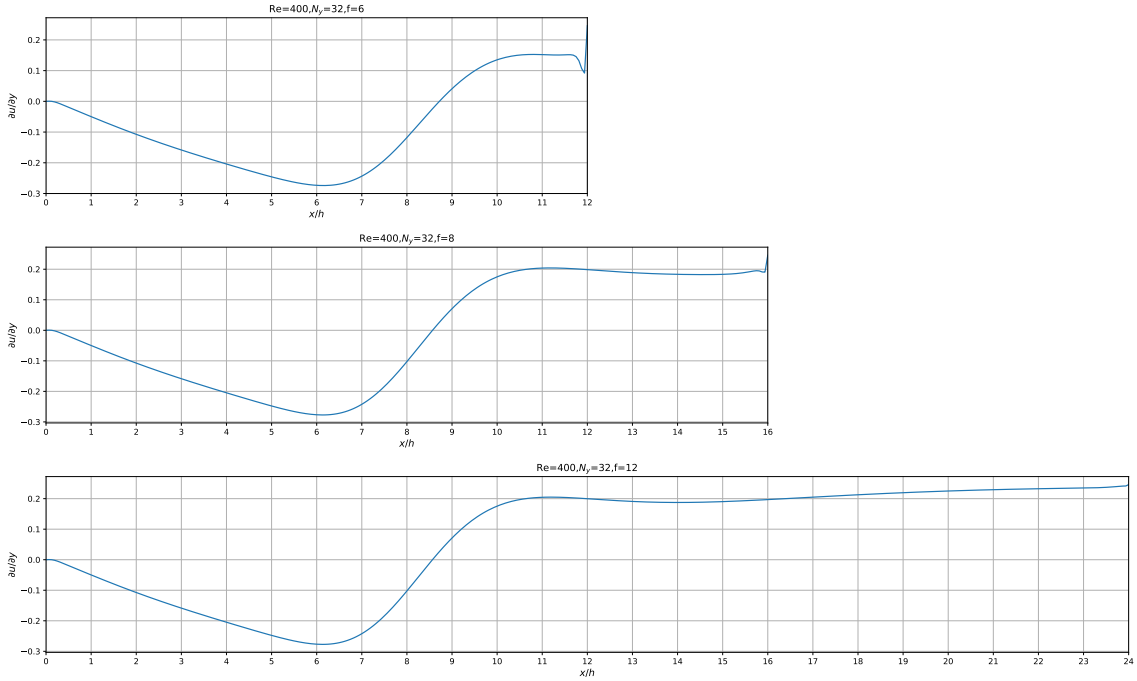

Figure 23. $\partial u/\partial y$ **of** $Re = 400$**,** $N_y = 16$**,** $f = 6, 8, 12$**.**

When running the $Re = 400$ cases, we can see that $f = 6$ is no longer adequate for the flow to become fully developed. As we can see in figure 20 and figure 22, the streamlines near the outflow boundary are jagged when $f = 6$ and $f = 8$. Note that this problem does have an impact on the re-attachment length, therefore when dealing with Reynolds numbers that are relatively large, we need to run our simulation on a longer domain.

In order to compare with Figure 13(b) in Armaly's paper, we plot the re-attachment length x_r versus the Reynolds number. As depicted in figure 24, the our x_r is in accordance with the result presented in Armaly's paper.

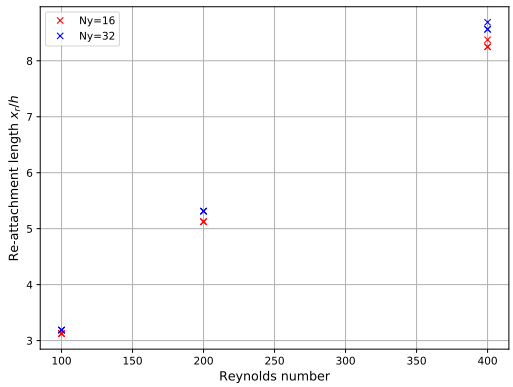

Figure 24. Re-attachment length x_r **versus the Reynolds number**

When running our code with different Reynolds numbers on different meshes, we found that as Re increases, it takes more iteration steps to obtain a converge solution. Meanwhile, not only does the higher mesh resolution slow down each iteration step, it also takes more iteration steps to reach the residual condition.